Thin Solid Films 730 (2021) 138706

Contents lists available at ScienceDirect

Thin Solid Films

journal homepage: www.elsevier.com/locate/tsf

The effect of dislocation-related V-shaped pits preparation on the strain of AlN templates

Xingyu Zhou [a,b], Yiren Chen [a,*], Zhiwei Zhang [a], Guoqing Miao [a], Hong Jiang [a], Zhiming Li [a], Hang Song [a,*]

[a] State Key Laboratory of Luminescence and Applications, Changchun Institute of Optics, Fine Mechanics and Physics, Chinese Academy of Sciences, Changchun 130033, China

[b] University of Chinese Academy of Sciences, Beijing 100039, China

ARTICLE INFO

Keywords:
Epitaxial growth
Microstructure
Aluminum nitride template
Dislocation defects
Wet etching
Stress regulation
Metal-organic chemical vapor deposition

ABSTRACT

Herein, the dislocation defects of an aluminum nitride (AlN) template heteroepitaxially grown by metal-organic chemical vapor deposition are exposed by phosphoric acid etching. The effect of dislocation-related V-shaped pits preparation on the strain of AlN epilayer is intensively studied. The results show that the dislocation defect etching leads to a strain gradient elongating along the growth direction of AlN and alleviates its initial tensile strain. Through a secondary epitaxy on the dislocation-etched AlN, it further reveals that the strain evolves into compressive strain state accompanied by surface cracking inhibition. It provides an effective way of stress regulation by dislocation-related etching and can be developed as a mask-free lateral epitaxial growth technique for high-performance AlN template preparation.

1. Introduction

As a direct wide and tunable bandgap semiconductor, aluminum gallium nitride (AlGaN) material has been used as the core material for developing deep ultraviolet (DUV) optoelectronic devices, such as DUV light-emitting diodes for environmental disinfection and public health in COVID-19 epidemic and solar-blind photodetectors for corona leakage detection in the field of ultra-high voltage power grids [1, 2]. Due to the absence of homogeneous substrates, the aluminum nitride (AlN) monocrystalline substrate is regarded as the ideal substrate for the preparation of AlGaN-based DUV optoelectronic materials. However, to date, it has been heavily restricted by its size and price under the existing mainstream physical vapor transport method such as sublimation-recondensation [3]. The heteroepitaxial growth of AlN on a lattice-mismatched sapphire substrate (so-called the AlN template) by metal-organic chemical vapor deposition (MOCVD) has been thus extensively developed as an alternative in the field of DUV optoelectronic devices [4, 5]. Unfortunately, although the sapphire acted as a heterogenous substrate, it has the advantages of low cost, availability in large dimension and transparency in the full UV-band perfectly meeting the operational waveband of the AlGaN material. However, there are some drawbacks that hinder the quality of AlN templates, mainly including the large lattice and thermal mismatch between AlN and sapphire, poor migration capacity of aluminum atoms on the sapphire surface as well [6]. These lead to a large density of dislocation defects and strong strain in the AlN templates. It is of great significance to disclose the relationship between dislocation defects and strain in the heteroepitaxial AlN templates, which will have a vital role for the optimal growth of AlN templates.

Herein, the comparative experiments of the AlN templates heteroepitaxially grown by different processes are carried out at first. The influence of dislocation-related V-shaped pits preparation on the strain of the AlN template is then demonstrated in detail. The related research is potential to develop a mask-free lateral epitaxial growth of AlN template by secondary epitaxy on the surface of V-shaped pits.

2. Experimental procedure

2.1. Detailed epitaxial growth of AlN template by continuous growth pattern

The AlN templates were grown on 2 in. c-plane sapphire substrates by MOCVD using the different processes. In the process of epitaxial growth, trimethylaluminium and ammonia (NH_3) were used as Al and N

* Corresponding authors
E-mail addresses: chenyr@ciomp.ac.cn (Y. Chen), songh@ciomp.ac.cn (H. Song).

https://doi.org/10.1016/j.tsf.2021.138706
Received 12 January 2021; Received in revised form 19 April 2021; Accepted 21 April 2021
Available online 24 April 2021

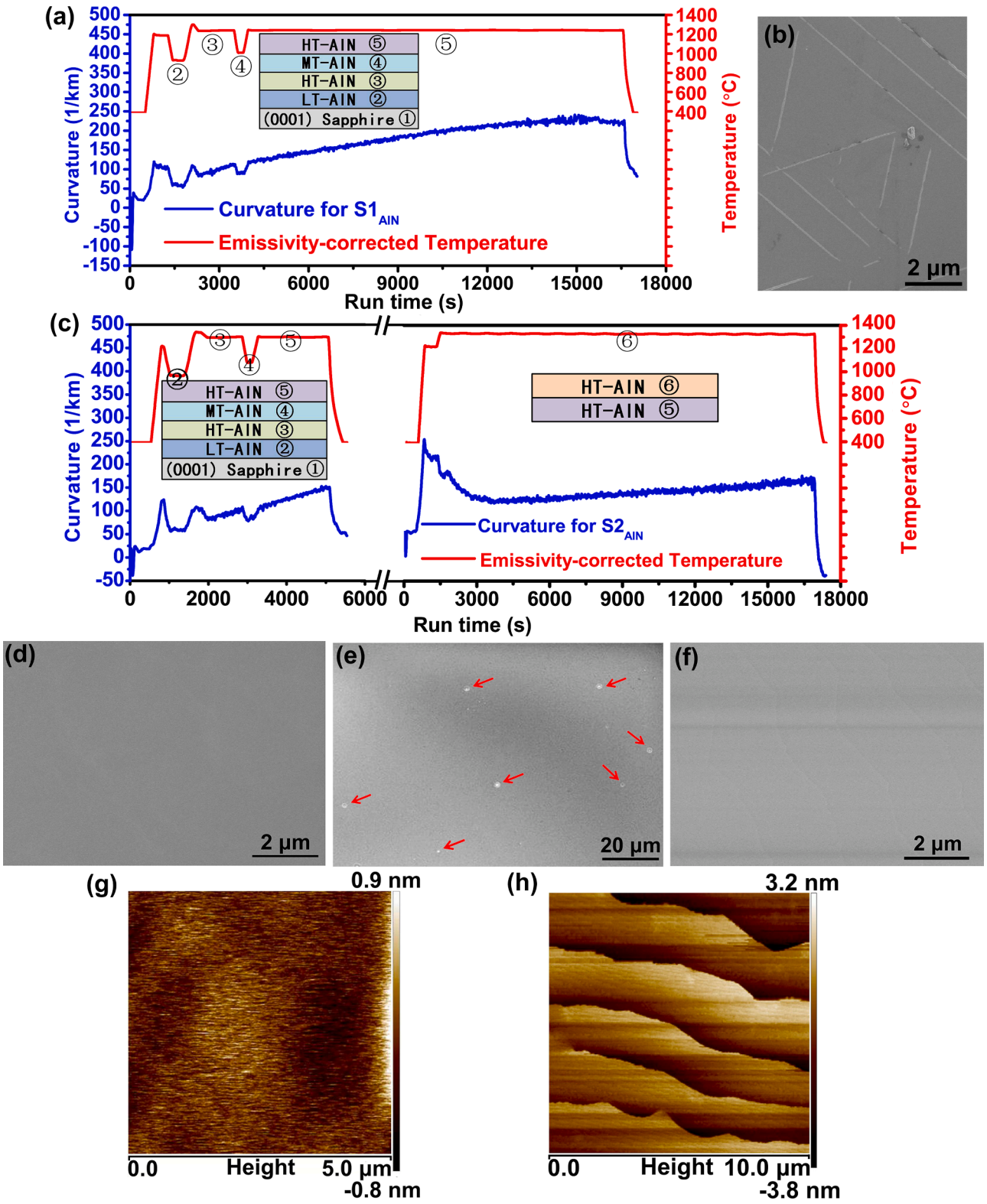

Fig. 1. (a) Transients of curvature and emissivity-corrected temperature for continuous growth of AlN. (b) The surface morphology of $S1_{AlN}$. (c) Transients of curvature and emissivity-corrected temperature for two-stage growth of AlN. The surface morphologies of $S2_{AlN}$ at (d) primary epitaxy, (e) after H_3PO_4 etching, and (f) secondary epitaxy. (g) AFM image for $S2_{AlN}$ at primary epitaxy stage. (h) AFM image of $S2_{AlN}$ at secondary epitaxy stage.

precursors while hydrogen as the carrier gas. The continuous growth pattern was based on the conventional two-step growth method with a thin mesothermal (MT-AlN) interlayer. In Fig. 1(a), the schematic layers (inset) identified by numbers correspond to the different growth stages marked with the same numbers strictly. The growth commenced with the sapphire substrate thermally desorbing at 1200 °C under a hydrogen atmosphere for 60 s. Then, a 36 nm-thick low-temperature AlN (LT-AlN) nucleation layer (NL) was deposited on the sapphire at about 950 °C with a reactor pressure of 5 kPa and a V/III ratio of about 2000. Subsequently, the growth temperature was risen up to 1330 °C with a ramp

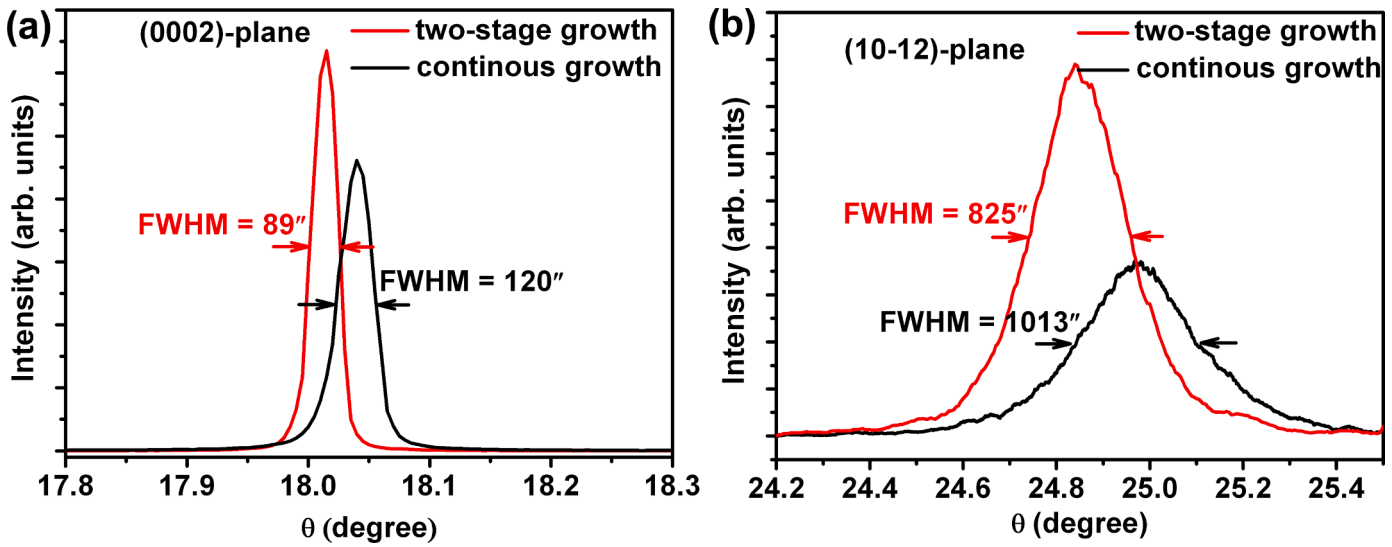

Fig. 2. The rocking curves of the (0002) and (102) planes for the two samples.

rate of 1.2 °C/s. During this process, the LT-AlN NL was recrystallized under the NH_3 atmosphere. After then, an about 240 nm-thick high-temperature AlN (HT-AlN) epilayer was grown at 1300 °C with a reactor pressure of 4 kPa and a V/III ratio of about 200. Subsequently, a 60 nm-thick MT-AlN interlayer was grown at 1050 °C with a V/III ratio of about 700 and a reactor pressure of 4 kPa. Finally, an about 1.5 μm-thick HT-AlN epilayer was grown at the same conditions of 240 nm-thick HT-AlN. The whole material then cooled down to room temperature naturally.

2.2. Detailed epitaxial growth of AlN template on two-stage growth pattern

The two-stage growth pattern included primary epitaxy and secondary epitaxy on etched AlN, as shown in Fig. 1(b). The primary epitaxy process was the same as the continuous growth pattern mentioned above. The only difference was that the thickness of the HT-AlN layer grown after the MT-AlN layer was only 370 nm. Before the secondary epitaxy, the primary epitaxial AlN was firstly etched by 85 wt % phosphoric acid (H_3PO_4) solution to form V-shaped pits located at the dislocation defects and then cleaned for secondary epitaxy (for details, see below). During the process of secondary epitaxy, the etched AlN template was thermally desorbed at 1200 °C under a hydrogen atmosphere for 480 s. After then, an about 1.6 μm-thick HT-AlN epilayer was grown at 1300 °C with a reactor pressure of 4 kPa and a V/III ratio of about 200. Finally, the sample was allowed to naturally cool down to room temperature.

2.3. Wet etching of primary epitaxial AlN

In the part of wet etching primary epitaxial AlN, the H_3PO_4 solution with a concentration of 85 wt% was used as the etching agent. It was conducted at a constant temperature of 80°C for 100 min to ensure that the dislocation defects of AlN were etched. Before carrying out secondary growth, the etched AlN template was cleaned with low concentration sodium hydroxide solution, deionized water, acetone and isopropanol in sequence. Then, it was dried in a nitrogen atmosphere at 150°C for 60 min. Finally, it was desorbed by inductively coupled plasma for 2 min at a power of 200 W to further clean its surface.

2.4. Characterization

We used an *in-situ* optical monitoring system (LayTec AG) to record the transients of curvature and temperature during the epitaxy. A scanning electron microscope (SEM, Hitachi S4800) and an atomic force microscope (AFM, Veeco multi-mode) were used to characterize the surface morphology of AlN. The SEM was operating at a voltage of 5 kV. The asymmetrical reciprocal space mapping (RSM) images around (105) reflection of AlN were characterized by a high-resolution X-ray diffractometer (XRD, Bruker D8) with a Cu $K\alpha_1$ radiation of 1.5406 Å, which was operating under a voltage of 40 kV and a current of 40 mA. For the asymmetric crystalline plane, a slight incidence mode was adopted during the XRD measurement. The room-temperature stress state was analyzed by Raman scattering spectra which were recorded in backscattering geometry with a 532 nm laser (LAS-532-100-HREV, HORIBA) as the excitation source.

3. Results and discussion

The comparative experimental results of the AlN templates hetero-epitaxially grown by different processes are shown in Fig. 1. All detailed growth information can be referred to in Experimental Section. In Fig. 1 (a), it presents the transients of curvature and emissivity-corrected temperature for the continuous growth pattern. The evolution of curvature for this AlN sample (labeled as $S1_{AlN}$) gradually increases from 85 km^{-1} (c1) to 235 km^{-1} (c2), and then levels off. The lattice mismatch and the different thermal expansion coefficients between substrate and AlN lead to the upward tendency of curvature. The change of constant curvature increase (bowing of curvature transient) proves ongoing relaxation process during growth. The curvature leveling off at c2 represents the onset of cracking visible in increasing scatter of curvature data, which can deduce that the AlN epilayer releases strain thoroughly through visible cracking after c2. The surface morphology with plenty of cracks in Fig. 1(b) is a good illustration of our deduction. In Fig. 1(c), it shows the preparation of AlN ($S2_{AlN}$) by a two-stage growth pattern, in which the primary epitaxy is similar to that of $S1_{AlN}$. In this stage, the evolution of curvature gradually increases from 60 km^{-1} (c3) to 150 km^{-1} (c4). The related surface morphologies are shown in Fig. 1(d) and (g), which present a smooth surface with a root-mean-square (RMS) roughness of 0.13 nm for a scan area of 5 × 5 μm^2. The pre-grown AlN is etched to form dislocation-related hexagonal V-shaped pits (denoted by red arrows in Fig. 1(e)). The secondary epitaxy is carried out on the etched AlN. In this stage, the evolution of curvature is also shown in Fig. 1(c), which undergoes a process of decreasing from a high level of 180 km^{-1} (c5) to a low one of 120 km^{-1} (c6), and then slowly increasing to 160 km^{-1}. The secondary epitaxial AlN presents a crack-free surface and has clear atomic steps with an RMS roughness of 0.867 nm in a scan

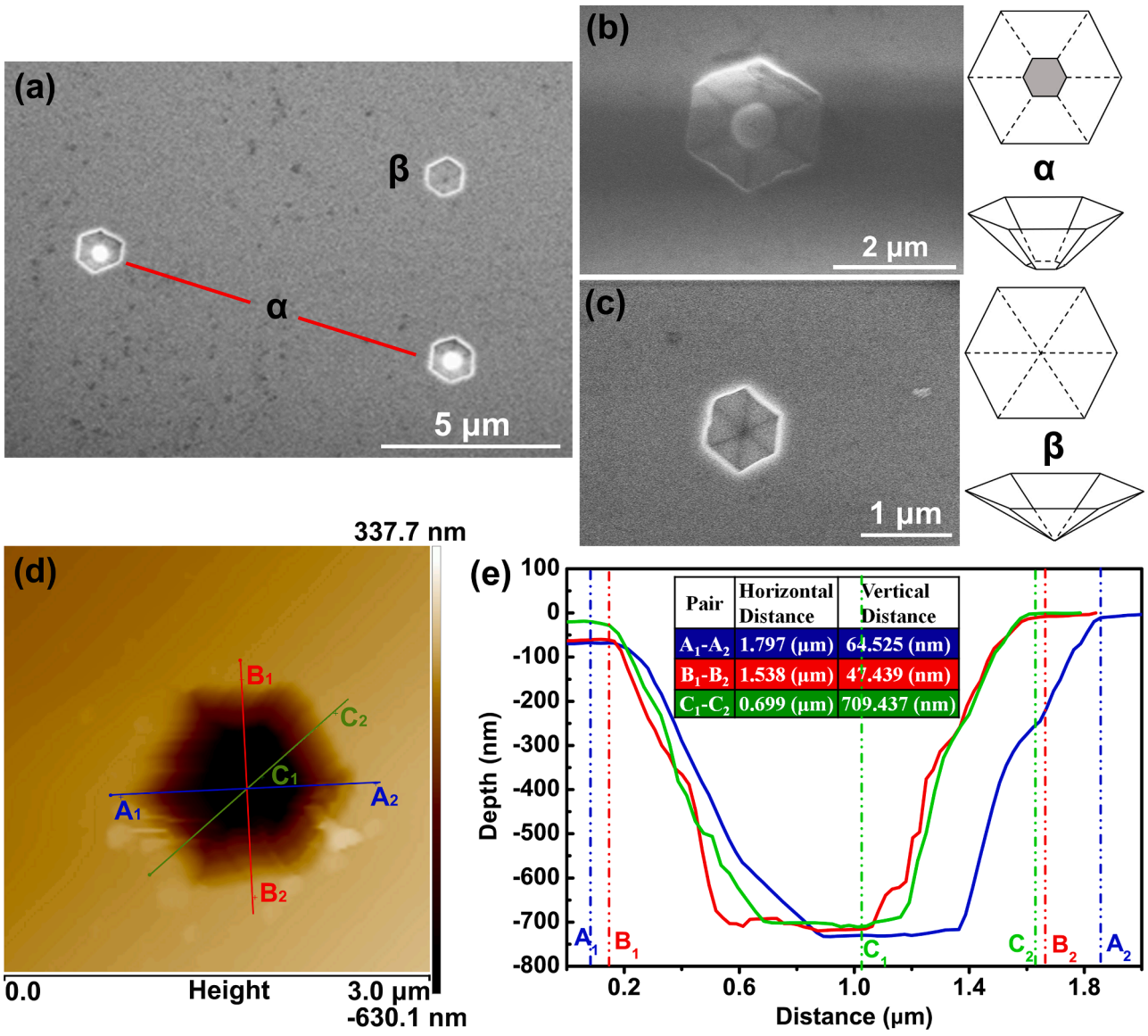

Fig. 3. (a) SEM image of V-shaped pits on AlN surface. (b) and (c) V-shaped pits with two main geometric structures. (d) AFM image for a typical α-type V-shaped pit. (e) The dimensions of the α-type V-shaped pit.

area of 10 × 10 μm^2, as shown in Fig. 1(f) and (h).

In addition, the rocking curves of the (0002) and (102) planes for the continuously grown AlN template and the AlN grown on etched template (two-stage growth one) with the same thickness are presented in Fig. 2(a) and (b). The full width at half maximum (FWHM) values of (0002) plane and (102) plane for the two-stage growth one are about 89 arcsec and 825 arcsec while those for the continuous growth one are about 120 arcsec and 1013 arcsec. As is well known, the FWHMs of (0002) plane and (102) plane rocking curves are usually used to evaluate the screw and edge dislocations of the epitaxial material. In the case of randomly distributed dislocations, the screw dislocation density (ρ_s) and the edge dislocation density (ρ_e) can be evaluated to be 1.71 × 10^7 cm^{-2} and 6.96 × 10^9 cm^{-2} for the two-stage growth one, 3.13 × 10^7 cm^{-2} and 1.04 × 10^{10} cm^{-2} for the continuous growth one using the existing evaluation method [6, 7]. This means that the quality of the two-stage growth one is improved.

The improvement can be ascribed to the strain regulation by preparing dislocation-related V-shaped pits on primary epitaxial AlN. Fig. 3 (a) presents the enlarged surface morphology of Fig. 1(e). As is well known, the wet chemical etching is a common technique for investigating surface defects of semiconductors [8, 9]. Therefore, a series of hexagonal V-shaped pits are formed on the surface of AlN after wet etching, whose locations originate from the dislocations of AlN. The dimension and geometric structure of the V-shaped pits tightly depend on the solution temperature and the etching time in the experiment, which has been detailedly studied in ref. 10. As can be seen, there are mainly two types of V-shaped pits screw (α) and edge (β) observed. The α-type V-shaped pit in Fig. 3(b) presents a hexagonal inverted trapezoidal shape while the β-type one in Fig. 3(c) is in a hexagonal inverted pyramid-like shape, both of which are comparable to Ravi et al. reported in 2018 [11]. The AFM image and its dimension for a typical α-type V-shaped pit are illustrated in Fig. 3(d) and (e), respectively. Its lateral size is statistically evaluated to be ranging from 1.5 μm to 1.7 μm, and the etching depth is about 709 nm, which is consistent with the thickness of the primary epitaxial AlN. This means that the dislocation is completely etched away by acid in the α-type V-shaped pit. In the β-type V-shaped pit, the etching depth is insufficient to penetrate the dislocation of AlN.

In order to analyze the effect of the dislocation-related V-shaped pits of the heteroepitaxial AlN template on its strain, the strain evolutions

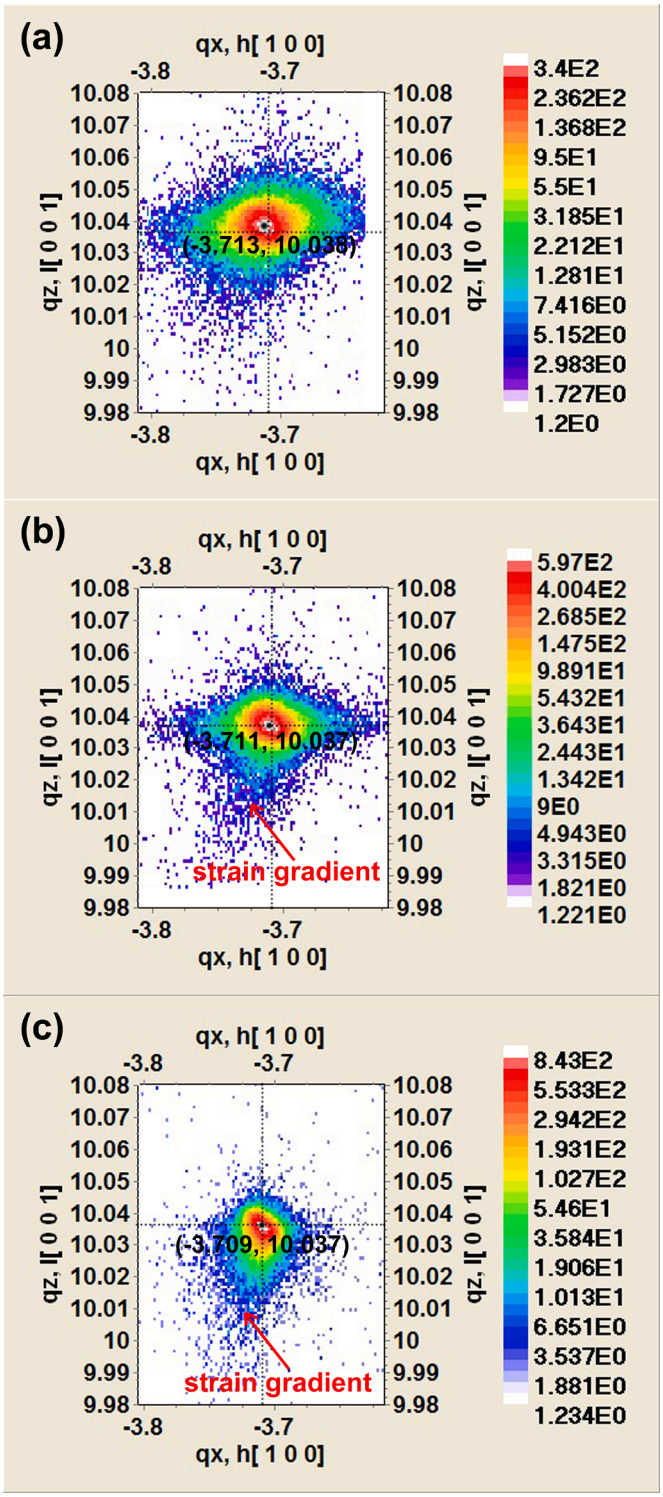

Fig. 4. The typical RSM images around (105) reflection for AlN. (a) primary epitaxy, (b) after etching, and (c) secondary epitaxy.

before and after the special treatment are studied. As seen in Fig. 4(a) to (c), they present the typical asymmetrical RSM images around (105) reflection for AlN under the conditions of as-grown, after H_3PO_4 etching, and secondary epitaxy on etched AlN, respectively. The asymmetrical RSM is an effective way to evaluate the strain characteristic of the heteroepitaxial semiconductor. In each RSM image, a well-resolved main peak with a series of contour lines is presented. The coordinates q_x and q_z are in directions parallel and vertical to the AlN epilayer surface. The reciprocal lattice point (RLP) denoted as (q_x, q_z) for fully relaxed AlN can be calculated as (-3.71, 10.037) for its (105) reflection by the lattice constant functions [12]. In Fig. 4(a), the RLP of the main peak for the as-grown AlN is measured as (-3.713, 10.038). In comparison with full relaxed AlN, the deviation in $q_x$direction indicates the as-grown AlN suffers from tensile strain caused by the lattice mismatch to the substrate. In Fig. 4(b), the RLP for the peak of the etched AlN is measured as (-3.711, 10.037), which presents a reduction in tensile strain. In addition, the broadening of the low-intensity RSM component in the $q_z$direction indicates the formation of strain gradient elongating along the direction perpendicular to its surface. This result is related to the etched V-shaped pits destroying the dislocation defects of the AlN epilayer, and further alleviating its residual stress. As is known to all, in the heterostructure material system, it becomes energetically favorable to relieve mismatch strain by the formation of misfit dislocations at the heterointerface [13]. Once the dislocations begin to form and propagate at the heterointerface, strain relaxation is taken place in the epilayer [14]. Fig. 4(c) presents the RSM image of the secondary epitaxial AlN on the etched AlN. As can be seen, its RLP of the main peak is located at (-3.709, 10.037), indicating that a small compressive strain is beneficial to suppress the surface cracking of AlN. Moreover, the low-intensity RSM component around the peak is narrower than that of Fig. 4(a) and (b) which means the improvement of the crystal quality. The result can be originated from the mask-free lateral epitaxial growth of AlN during the secondary epitaxy on the V-shaped pits.

To further understand the effect of dislocation defects etching on film strain, the Raman spectra for primary epitaxy, after etching, and secondary epitaxy samples are presented in Fig. 5(a). In addition to the peaks of the (0001)-oriented sapphire, the spectra of three samples exhibit two other peaks, corresponding to the non-polar E_2(high) and polar A_1(LO) photon modes which are allowed for (0001)-oriented wurtzite structure AlN [6]. The unstrained phonon frequency of E_2(high) for AlN at room-temperature is located at 657.4 cm^{-1}. As shown in Fig. 5(b), as a main phonon mode, the E_2(high) peaks of the three samples are located at 654.45 cm^{-1},654.93 cm^{-1}, and 658.65 cm^{-1}, respectively, with a trend indicated by the dotted arrow. In fact, the frequency shift of the phonon mode is tightly related to the stress state in the heteroepitaxial material. Due to the existence of the residual tensile strain, the frequency of E_2(high) will shift to the lower side of the strain-free position. On the contrary, it will shift to the higher side due to the residual compressive strain. Therefore, the as-grown and after etching samples appear as tensile strain while the secondary epitaxy sample appears as compressive strain. However, the etched AlN has a slight frequency shift compared with the as-grown one, indicating the reduction of tensile strain due to the destruction of the dislocation defects. These results are quite in agreement with the RSM images mentioned above.

4. Conclusions

In summary, we prepare hexagonal V-shaped pits along the dislocation defects of heteroepitaxial AlN material by wet etching, and the effect of dislocation defects etching on its strain is intensively studied. The result shows that the destruction of dislocation defects forms strain gradient elongating along the growth direction of AlN and alleviates its initial tensile stress. During the secondary epitaxy process, the AlN epilayer evolves into compressive strain state accompanied by the improvement of crystalline quality due to the destruction of initial dislocation defects and the lateral epitaxial role of the V-shaped pit surface.

Credit Author Statement

Xingyu Zhou: Data curation, Writing-Original draft preparation. **Yiren Chen:** Conceptualization, Methodology, Data curation, Writing-Original draft preparation, Funding acquisition. **Zhiwei Zhang:**

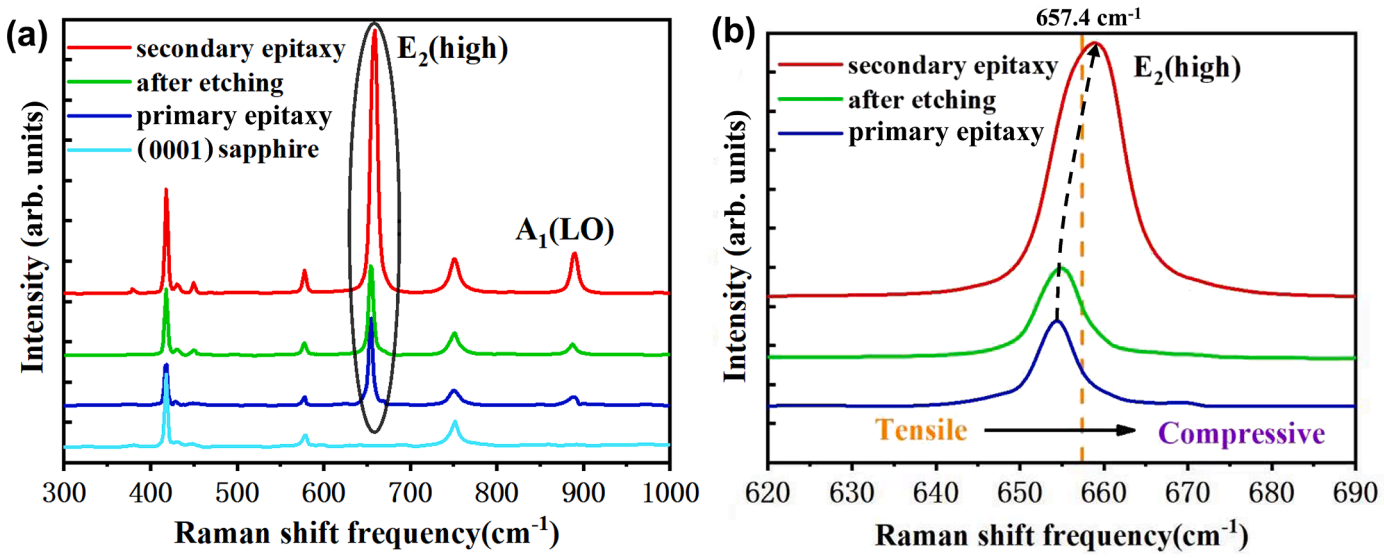

Fig. 5. (a) Raman spectra for comparison. (b) Enlarged image of the Raman spectra around E_2(high) peak.

Methodology, Investigation. **Guoqing Miao:** Validation, Resources. **Hong Jiang:** Project administration, Resources. **Zhiming Li:** Investigation, Visualization. **Hang Song:** Supervision, Funding acquisition.

Declaration of Competing Interest

The authors declare that they have no known competing financial interests or personal relationships that could have appeared to influence the work reported in this paper.

Acknowledgment

This work was supported by National Natural Science Foundation of China (Grant numbers 61504144, 51472230), and Department of Science and Technology of Jilin Province (Grant number 20170520156JH).

References

[1] M. Kneissl, T. Seong, J. Han, H. Amano, The emergence and prospects of deep-ultraviolet light-emitting diode technologies, Nat. Photonics 13 (2019) 233–244.
[2] Y. Chen, Z. Zhang, G. Miao, H. Jiang, Z. Li, H. Song, Epitaxial growth of polarization-graded AlGaN-based solar-blind ultraviolet photodetectors on pre-grown AlN templates, Mater. Lett. 281 (2020), 128638.
[3] T. Wunderer, C.L. Chua, J.E. Northrup, Z. Yang, N.M. Johnson, M. Kneissl, G. A. Garrett, H. Shen, M. Wraback, B. Moody, H.S. Craft, R. Schlesser, R.F. Dalmau, Z. Sitar, Optically pumped UV lasers grown on bulk AlN substrates, Phys. Status Solidi C 9 (2012) 822–825.
[4] J. Kim, J. Pyeon, M. Jeon, O. Nam, Growth and characterization of high quality AlN using combined structure of low temperature buffer and superlattices for applications in the deep ultraviolet, Jpn. J. Appl. Phys. 54 (2015), 081001.
[5] J. Yan, J. Wang, Y. Zhang, P. Cong, L. Sun, Y. Tian, C. Zhao, J. Li, AlGaN-based deep-ultraviolet light-emitting diodes grown on high-quality AlN template using MOVPE, J. Cryst. Growth 414 (2015) 254.
[6] Y. Chen, H. Song, D. Li, X. Sun, H. Jiang, Z. Li, G. Miao, Z. Zhang, Y. Zhou, Influence of the growth temperature of AlN nucleation layer on AlN template grown by high-temperature MOCVD, Mater. Lett. 114 (2014) 26–28.
[7] S.R. Lee, A.M. West, A.A. Allerman, K.E. Waldrip, D.M. Follstaedt, P.P. Provencio, D.D. Koleske, C.R. Abernathy, Effect of threading dislocations on the Bragg peakwidths of GaN, AlGaN, and AlN heterolayers, Appl Phys Lett 86 (2005), 241904.
[8] C. Flynn, L.W. Sim, Effects of phosphoric acid on the surface morphology and reflectance of AlN grown by MBE under Al-rich conditions, Thin Solid Films 589 (2015) 338–343.
[9] S.L. Qi, Z.Z. Chen, H. Fang, Y.J. Sun, L.W. Sang, X.L. Yang, L.B. Zhao, P.F. Tian, J. J. Deng, Y.B. Tao, T.J. Yu, Z.X. Qin, G.Y. Zhang, Study on the formation of dodecagonal pyramid on nitrogen polar GaN surface etched by hot H_3PO_4, Appl. Phys. Lett. 95 (2009), 071114.
[10] Y.H. Choi, K.H. Baik, R. Choi, J. Oh, J. Kim, Photo-enhanced acid chemical etching of high-quality aluminum nitride grown by metal-organic chemical vapor deposition, ECS J. Solid State Sci. Technol. 8 (2019). N42-N46.
[11] L. Ravi, B. Krishnan, Epitaxial growth of AlN microwalls on wet etched GaN template by MOCVD, Superlattice. Microst. 123 (2018) 144–153.
[12] Y.R. Chen, Z.W. Zhang, H. Jiang, Z.M. Li, G.Q. Miao, H. Song, The optimized growth of AlN templates for back-illuminated AlGaN-based solar-blind ultraviolet photodetectors by MOCVD, J. Mater. Chem. C 6 (2018) 4936–4942.
[13] D. Holec. P.M.F.J. Costa, M.J. Kappers, C.J. Humphreys, Critical thickness calculations for InGaN/GaN, J. Cryst. Growth 303 (2007) 314–317.
[14] A.E. Romanov, E.C. Young, F. Wu, A. Tyagi, C.S. Gallinat, S. Nakamura, S. P. DenBaars, J.S. Speck, Basal plane misfit dislocations and stress relaxation in III, -nitride semipolar heteroepitaxy 109 (2011), 103522.